Encapsulation, solid-phases identification and leaching of toxic metals in cement systems modified by natural biodegradable polymers

M. Lasheras-Zubiate, I. Navarro-Blasco, J.M. Fernández, J.I. Álvarez*

Department of Chemistry and Soil Sciences, School of Sciences, University of Navarra, c/ Irunlarrea, 1, 31008, Pamplona, Spain

Abstract

Cement mortars loaded with Cr, Pb and Zn were modified by polymeric admixtures (chitosans with low (LMWCH), medium (MMWCH) and high (HMWCH) molecular weight and hydroxypropylchitosan (HPCH)]. The influence of the simultaneous presence of the heavy metal and the polymeric additive on the fresh properties (consistency, water retention and setting time) and on the compressive strength of the mortars was assessed. Leaching patterns as well as properties of the cement mortars were related to the heavy metals-bearing solid phases. Chitosan admixtures lessened the effect of the addition of Cr and Pb on the setting time. In all instances, chitosans improved the compressive strength of the Zn-bearing mortars yielding values as high as 15 $N.mm^{-2}$. A newly reported Zn phase, dietrichite ($ZnAl_2(SO_4)_4 \cdot 22\ H_2O$) was identified under the presence of LMWCH: it was responsible for an improvement by 24% in Zn retention. Lead-bearing silicates, such as plumalsite ($Pb_4Al_2(SiO_3)_7$), were also identified by XRD confirming that Pb was mainly retained as a part of the silicate network after Ca ion exchange. Also, the presence of polymer induced the appearance and stabilization of some Pb(IV) species. Finally, diverse chromate species were identified and related to the larger leaching values of Cr(VI).

1. Introduction

The use of Portland cement (OPC) to immobilise hazardous wastes has become widespread because of their availability, versatility and low cost [1]. In particular, the immobilization of heavy metals by solidification/stabilization (S/S) is an effective method to reduce their hazard to the environment [2-4]. The incorporation of the waste into the hydrated cement system takes place through different mechanisms [5-7], encapsulation being one of the most important.

The contaminants included in the cement can, eventually, be transferred from this stabilized matrix to a liquid medium such as water or other solutions, this process being known as leaching. Both field and laboratory leaching studies are relevant to obtain information about the chemical speciation and the mobility of contaminants in the S/S process evidencing the associated potential risks [5,8].

The hydration of cement mortars is influenced by the presence of heavy metals. Some of the rheological properties may be also jeopardized [9-10]. Hardened state properties, such as compressive strength, can also undergo alteration upon addition of toxic metals. Zinc, for example, has been reported to strongly delay OPC hydration and to reduce the compressive strength [11], such as in the case of S/S of toxic ashes [12]. The literature abounds with proposed mechanisms to explain the effect of the heavy metals addition on the setting time of OPC mortars [10,13-16]. Changes in the fresh state properties and long-term stability of the cement mortars can have deleterious effects on the applicability and usefulness of cement mortars loaded with heavy metals. In order to minimize these adverse effects on the properties of the cement, mineral admixtures such as zeolites, metakaolin, bagasse ash, clinoptilolite [17-19] and polymeric admixtures, such as polycarboxylate ethers, naphthalene-based superplasticizers, latexes and acrylic polymers can be added to the cement mortars [8,13, 20-22]. One of this type of admixtures is chitosan, a natural biopolymer structurally analogous to some well-known cement cellulosic additives. Chitosans show remarkable complexing abilities for

heavy metals [23] and they have been proved to modify some of the cement properties [24-26]. In this case, noticeable results were obtained even when incorporated in a very low amount (i.e. 0.4 wt.% by cement) [26]. Although long-term biodegradation performance could be considered a hypothetical drawback, its influence on the cement mortar would be minimum given the scarce amount of the polymer in the total weight of the mortar.

The objective of the present paper is to bring information on the immobilization of Cr, Pb and Zn by cement mortars modified by the addition of an unexplored range of natural chitosan biopolymers. Fresh and hardened state properties of the metal-loaded mortars were also assessed with the aim of shedding light on the observed changes as a function of the added polymer. Identification of the chemical forms in the solid state of the retained metals was also carried out to gain understanding of the immobilization process of heavy metals in cement when polymeric additives were simultaneously present. The metals selected for this study were Pb(II), Cr(VI) and Zn(II), identified as priority metallic pollutants [13,23,27-29].

2. Experimental

2.1. Materials

Different molecular weights (MW) chitosans (LMWCH: 210 kDa; MMWCH: 470 kDa; HMWCH: 835 kDa) were used (Sigma-Aldrich). The synthesis of HPCH (119 kDa), was done according to Peng et al. [30]. Basic structures of the chitosan and the etherified derivative are shown in Fig. 1. The degree of substitution (DS) for HPCH was seen to be 11.24 by elemental analysis. The amount of residual chloride was also determined by potentiometric titration, resulting in 320 ppm. Taking into account the admixture dosage of 0.4% by cement weight, a negligible amount of chloride (< 2 ppm) was calculated to be incorporated by the polymer.

An OPC (CEM II32.5 N) and a standardized siliceous aggregate supplied by Instituto Eduardo Torroja (Spain), with a constant particle size distribution [31], were used to prepare the mortars.

The heavy metal load (1% of heavy metal/cement) consisted of $Zn(NO_3)_2$, $Pb(NO_3)_2$ (Merck) and $K_2Cr_2O_7$ (Panreac). Nitrate salts were chosen because of their solubility [32].

2.2. Mortar preparation

Cement, aggregate and chitosan (when necessary) were blended for 5 min with a mixer. Water was then added and mixed for 90 s at low speed. When required, one of the selected metal salts was dissolved in the mixing water in the aforementioned percentage. The binder:aggregate ratio (B:Ag) was 1:3, by weight, and the selected water:cement ratio was 0.55:1. These ratios yielded a control mortar with a good workability. Chitosans were added at a dosage of 0.4% of the cement weight and only one additive was added to each mortar to unequivocally evaluate their individual effect. Fresh mixtures were moulded in 40x40x160 mm casts and cured 28 days according to a norm [33] to evaluate the hardened state properties. Three specimens were prepared for each one of the mortar compositions, a total of 54 cement test pieces being assayed. Statistical significance of data was guaranteed by the adequate number (2 to 6) of replicates and/or instrumental measurements for the different assays.

2.3. Tests

2.3.1. Mortar properties

For the fresh state, several properties were studied: consistency through the flow table test, by measuring the slump of the mortar after 15 strokes on a specific compacting table [34]; water-retention capacity, determined by weighting absorbent materials placed on the fresh sample before and after 5 min of contact under pressure [35]; and setting time, obtained from a specific

98 device provided with a bradawl, which pushed the fresh sample until the strength exerted to
99 introduce it into the sample was larger than 15 N [36].

100 In hardened specimens, compression strength tests were executed on a Proeti ETI 26.0052 at a
101 loading rate of 50 $N \cdot s^{-1}$. Pore size distributions were obtained by mercury intrusion porosimetry
102 (MIP) using a Micromeritics AutoPoreIV9500 with a pressure ranging between 0.0015 and 207
103 MPa.

104

105 2.3.2. Identification of the heavy metals compounds in the solid state

106 The mineralogical phases were determined by X-ray diffraction (XRD) in a Bruker D8Advance
107 diffractometer (Karlsruhe, Germany), with a $CuK_{\alpha 1}$ radiation and 0.02º 2θ increment and 1
108 $s \cdot step^{-1}$, from 2º to 90º 2θ.

109 Scanning Electron Microscopy (SEM), Backscatter Scanning Electron (BSE) and Electron
110 Dispersion Analysis of X-ray (EDS) (HITACHI, S-4800) were used for microscopic
111 observations, local composition and mapping of the metals distribution.

112 X-ray fluorescence (XRF) was coupled with an optical microscope to collect additional data on
113 the chemical composition of selected areas of the samples.

114

115 2.3.4. Leaching tests

116 A semi-dynamic Tank Test [37] already described [24] was used. Test pieces (40 mm x 37 mm
117 cylinders) were prepared by duplicate, moulded and cured as explained in section 2.2. A total of
118 36 cement blocks were analysed and the results were the average of three instrumental
119 measurements.

The above mentioned whole sample was placed in sealable 110x110x110 mm methacrylate tanks. These tanks were filled with 1L of demineralized neutral pH water as leaching fluid. After the indicated period, all the leachate was drained off and filtered through a 0.45 μm-pore size nylon membrane (CHMLAB Group). Conductivity and pH were measured with a 4-Star benchtop pH/conductivimeter. A 10 mL aliquot of each sample was stored in sub-boiling HNO_3 to quantify the leached metals. Afterwards, the tank was filled again with the same volume of water, and the procedure repeated. Eluates were collected at eight different times (0.25, 1, 2.25, 4, 9, 16, 36 and 64 days).

A Perkin-Elmer AAnalyst 800 atomic absorption spectrometer was used to measure the concentration of leached metals under usual instrumental settings [24].

From the data collected, the measured cumulative leaching for each component was calculated using the following equation well described in the norm for leaching of monolithic materials [37]:

$$\varepsilon_n^* = \sum_{1=n}^{n} E_i^* \quad \text{for } n=1 \text{ to } N \qquad (1)$$

where ε_n^* is the measured cumulative leaching of a component for a period N comprising fraction i=1 to n in mg m^{-2}, E_i^* is the measured leaching of the component in fraction i in mg m^{-2} and N is the number of replenishing periods.

Derived cumulative leaching was also calculated according to the formula:

$$\varepsilon_n = \frac{\left(E_i^* \times \sqrt{t_i}\right)}{\left(\sqrt{t_i} - \sqrt{t_{i-1}}\right)} \quad \text{for } n=1 \text{ to } N \text{ (where } i=n) \qquad (2)$$

where ε_n is the derived cumulative leaching of a component for a period *N* comprising fraction *i*=1 to *n* in mg m^{-2}, E_i^* is the measured leaching of the component in fraction *i* in mg m^{-2}, t_i is the replenishing time of fraction *i* in s and t_{i-1} is the replenishing time of fraction *i-1* in s.

Leaching mechanism was determined from the slope of the linear regression analysis (log-log plots of cumulative leaching vs. time) through the eight data points, considered in different increments of time, as detailed in the EA NEN 7375:2004 norm [37]. Criteria for the interpretation of the different slope values can also be found in the quoted norm and in some previous works [7]: gradients below 0.35 indicated surface wash-off (in the case of increment from 0.25 to 4 days) or depletions (for all the rest of time increments); when the gradient was between 0.35 and 0.65 the mechanism was diffusion (for all the studied time intervals), whereas values higher than 0.65 indicated delayed diffusion (interval from 0.25 to 4 days) or dissolution (for all the rest of time increments) [7,37].

The negative logarithm of the effective diffusivity (pDe) was calculated as an indicator of the leaching rate for each metal, according to the following equation that can be found in the EA NEN 7375:2004 norm [37]:

$$D_e = \left(\frac{\varepsilon_{64}}{2653 \cdot \rho \cdot U_{avail}} \right)^2 \cdot f \qquad (3)$$

Where De is the effective diffusion coefficient ($m^2 s^{-1}$), ε_{64} is the derived cumulative leaching after 64 days (mg m^{-1}), ρ is the density of the specimen (kg m^{-3}), U_{avail} is the leachable available quantity of the component in mg per kg of dry matter and f corresponds to a unitary value (s^{-1}).

As reported in the criteria of the norm [37] and in previous works such as that of Malviya and Chaudhary [7], the higher the pDe, the lower was the leaching rate. Values below 11.0 indicated

high mobility, results between 11.0 and 12.5 indicated average mobility and values above 12.5 indicated low mobility of the component.

3. Results and discussion

3.1. Fresh state properties

In polymer-free mortars, as proved by the measured slump (Fig. 2), Cr caused a fluidity reduction of *ca*. 6% while Pb provoked a flowability increase of around 3%. Results obtained for Zn were markedly different: the mixture was particularly heterogeneous and disaggregation was as large as to prevent slump measurements.

Native chitosan-modified mortars showed the above mentioned general trend. However, the addition of HPCH cancelled out the effect of the metal addition, giving rise to a slump diameter very close to that of the metal-free mortar (Fig. 2). In Zn-bearing samples, incorporation of HPCH yielded less disaggregated mixtures, although not consistent enough to be measured in the slump tests.

Water retention of plain cement mortar was not altered by incorporation of either Cr or Pb, irrespective of the presence or absence of chitosans (Fig. 3). Conversely, the presence of Zn consistently increased the water retained in the mortars by ca. 15%. This phenomenon could be related to the reported formation of calcium hydroxyzincate ($CaZn_2(OH)_6.2H_2O$) [38] that results in a withdrawal of both calcium and hydroxyl ions from solution, thus hindering the CSH gel formation. As a consequence, a larger non-combined water ratio remains in the fresh paste as proved by the higher water retention values. Furthermore, the delay in the CSH gel formation causes the fresh cement paste to become lumpy.

Experimental results showed that the addition of heavy metals gave rise to major changes in the setting time (Fig.4). Cr-bearing mortars reduced their setting time by 45%, while Pb-bearing mortars increased it by 20%. It is noteworthy that Pb-bearing mortars prepared for hardened state measurements could not be de-moulded in the first week, thus confirming the retarding effect on the hydration of this metal. The heterogeneous consistency of the mortar in the presence of Zn hampered the experimental measurements although the observed non-formation of the CSH gel points to a strong delay in the setting time. The delay observed for Zn-bearing cements has controversially been ascribed [11] to the formation of either a gelatinous layer of $Zn(OH)_2$ or the formation of the above mentioned $CaZn_2(OH)_6.2H_2O$ [38].

Hydrolysis of plumbite species (PbO_2^{2-}) has been invoked for the clear retarding effect of Pb [38], whereas results for Cr-bearing cements vary from a shortened setting time [39] to a longer setting period [40-41].

In our case, chitosan admixtures lessened the effect of both Cr and Pb to a considerable degree and, as a matter of fact, the values of the setting time resembled those of the metal-free mortar. Thus, the addition of HMWCH to Cr-bearing samples increased the workable life from 202 min of the polymer-free sample to 322 min and so the polymer cancels out the effect of the chromium incorporation. On the other hand, the addition of HMWCH, MMWCH and LMWCH in Pb-bearing samples reduced the setting time from 442 min (for the polymer-free Pb-bearing sample) to ca. 350 min, again obviating the effect on the setting time caused by Pb. The etherified derivative, HPCH, had a similar lessening effect: for Cr-bearing samples, HPCH increased the workable life from 202 min to 247 min; for Pb-bearing samples, the setting time underwent a reduction from 442 min to 322 min. Results highlight that the addition of chitosans as cement admixtures favourably overcame the deleterious effects caused in setting time by the presence of either Cr or Pb in loaded mortars. These findings point to the technical usefulness of these admixtures in improving the performance of heavy-metal loaded OPC mortars.

207

208 3.2. Hardened state properties and chemical identification of the heavy metals in different solid
209 state phases

210 Compressive strength tests were carried out as a good assessment of the S/S processes of heavy
211 metals in a cement-based matrix. A minimum value of compressive strength is desirable in
212 order to guarantee the retention of the wastes in the solid phase [42]. This value has been
213 established by the US EPA [43] as 0.34 $N \cdot mm^{-2}$ for the unconfined compressive strength in
214 cylindrical cement specimens for a stabilized/solidified material, that has become widely
215 recognised and used [44]. Experimental results for polymer-free mortars (Fig. 5), showed that
216 measurements in Zn-bearing samples could not be made due to the fresh state disaggregation of
217 the matrix, rendering the compressive strength values close to zero, not complying with the
218 above mentioned minimum compressive strength value. On the other hand, the addition of Cr
219 increased the compressive mechanical strength by 8%, phenomenon related to the improved
220 crystal growth of ettringite [45]. Finally, the addition of Pb resulted in a 30% increase of the
221 compressive strength justified by a reported reduction of the porosity of the mortars [11,42].

222 The addition of chitosans in Cr-loaded mortars provoked, in general, a statistically non-
223 significant reduction in the compressive strength yielding values similar to those in the
224 reference metal-free and polymer-free mortar. The HPCH addition gave rise to the most marked
225 reduction (ca. 21% drop) in strength that was related to the increase in the 1μm-diameter pore
226 fraction observed in MIP measurements (Fig. 6). However, the addition of the other polymers
227 did not significantly alter the pore distributions (Fig. 6). Presence of chitosans in Pb-bearing
228 samples did not modify the strength of the mortars to a great extent (variations from the
229 polymer-free sample were within ± 15% of variation in the strength). The marked reduction
230 observed in LMWCH samples (strength loss of 6.2 $N \cdot mm^{-2}$, 18% reduction in strength) was in

line with the larger amount of pores measured for the corresponding sample, especially for 0.2 μm diameter pores.

As for Zn, literature had already alerted to dramatic reductions of the compressive strength of the Zn-doped cements [11,46]. The lack of CSH gel formation led to the observed large porosity of these Zn-doped cements (see Fig. 6), thus explaining the strong reduction in the mechanical strength (virtually zero). However, it is noteworthy that the addition of any of the employed chitosans rendered the compressive strength measurable, as seen in Fig. 5. By way of example, upon the addition of MMWCH and HMWCH, the compressive strength reached values beyond 15 $N \cdot mm^{-2}$. In all instances, the incorporation of chitosans yielded mortars with compressive strength values well over the minimum established by the norm [43]. Additionally, Fig. 6 shows a clear reduction in porosity in Zn-loaded mortars when any of the assayed polymers were present.

This rise in strength is a remarkable feature when compared to the polymer-free sample, and it means that the handling and applicability of the cement-based mixtures loaded with Zn are greatly improved.

The chitosan polymers seem to play a double role. On the one side, they provide a structurally reinforced cement matrix and, on the other side -and much more relevant-, the polymers sequestrate water avoiding the formation of calcium hydroxy-zincates while favouring the CSH gel formation. As a matter of fact, in the polymer-free Zn-doped mortar, $CaZn_2(OH)_6 \cdot 2H_2O$ was observed by means of XRD measurements (main diffraction peak: 28.6 º 2θ) as well as a noticeable amount of C_2S that remains unhydrated (Fig. 7a). This definite finding points to the specific phase responsible for the delay in the setting time in the presence of Zn in polymer-free mortars [11,38].

When those same Zn-loaded mortars were modified by the addition of chitosan polymers, they did show neither that calcium hydroxy-zincate phase nor the anhydrous C_2S. Additionally, the formation of CSH resulted in a porosity decrease (Fig. 6). Furthermore, XRD measurements carried out in chitosan-modified Zn-loaded cements did show other crystalline Zn-phases. For example, the addition of MMWCH originated $Zn(OH)_2$, which could be identified by its peaks at 27.32º, 27.26º and 29.46º 2θ. A newly identified compound, dietrichite ($ZnAl_2(SO_4)_4 \cdot 22H_2O$; main peak: 20.50º 2θ) was found in the LMWCH-treated specimen (Fig. 7a). Supporting these results, SEM-EDS mapping images showed that Zn was heterogeneously retained in the sample, specially associated to Ca and/or Al (also Fe-bearing) compounds (Fig. 8). These findings are in excellent agreement with the main crystalline phases identified by XRD. These results were also confirmed by XRF analysis, in which Zn was seen to be irregularly distributed in spots and incorporated to Ca and also Fe-bearing compounds. The low atomic weight of the Al prevented its identification by XRF, but the spectra clearly showed Ca, Fe and Zn together with small amounts of Si (Fig. 9). These experimental findings indicate that Zn was retained by forming specific phases as those above mentioned rather than by the formation of a Zn substitutional compound in the hydrated calcium silicate network.

From this Zn-bearing phase characterization, we conclude that the observed setting time delay and the large water retention values were due to either the action of the calcium hydroxy-zincate or the dietrichite formation, which results in: (i) a retention of a considerable number of water molecules (22 per molecular weight unit); and (ii) a withdrawal of aluminium, responsible for the early stage of the setting through the C_3A that controls the type and amount of the hydration products. It must be taken into account that C_3A quickly dissolves after addition of water to the anhydrous cement. Even if sufficient sulphate ions are provided, the formation of ettringite takes place by reaction between aluminium and sulphate ions, in the well-known flash setting process [47].

279 New silicates and aluminosilicates forms involving Pb apart from leadhillite
280 ($Pb_4SO_4(CO_3)_2(OH)_2$) that had already been reported [48] were identified by XRD in all the
281 studied samples. The new silicate-based phases, of very close composition, were of the
282 following type: plumalsite ($Pb_4Al_2(SiO_3)_7$, main peaks: 21.77º, 18.09º 2θ); lead silicate
283 ($Pb_3Si_2O_7$, peaks: 24.80º, 20.60º 2θ); lead silicate hydrate ($Pb_2SiO_4 \cdot xH_2O$, peak: 24.80º 2θ) and
284 alamosite ($PbSiO_3$, peaks: 25.00º, 25.17º 2θ ; Fig. 7b). These findings clarify the existing
285 controversy on the fixation mechanism of Pb [49] by proving that the majority of lead was
286 retained as a part of the silicate network formed after substitution for calcium ions, rather than a
287 simple encapsulation of the metal hydroxide in a silicate matrix. Up to now, no crystalline form
288 of this type of lead silicates had ever been confirmed and identified by XRD [48,50]. In support
289 of our findings, SEM-EDS and BSE-image observations showed a homogeneous lead
290 distribution all over the cement matrix. The mapping of chemical elements confirmed that Pb
291 was regularly distributed along the calcium silicate network, associated with Si and Ca presence
292 (Fig. 10).

293 Additionally, in those samples in which different polymeric chitosan-based additives were
294 added, several Pb(IV) species were found: K_4PbO_4 (diffraction peaks: 28.77º, 29.47º 2θ, in the
295 LMWCH sample, Fig. 7b), Ca_2PbO_4 (peaks 17.70º,18.20º 2θ in MMWCH specimen) and PbO_2
296 (peaks: 28.44º,23.26º 2θ). The surge of these Pb(IV) species is a novelty because, in all
297 instances, lead had always been mentioned to be in the Pb(II) state. Furthermore, the formation
298 of PbO_2^{2-} species was said to be responsible for the retarding action caused by the lead presence
299 as in the case of the calcium hydroxy-zincate [38]. The occurrence of Pb(IV) species in the solid
300 state, according to the chemical composition of the XRD data, might be explained by both the
301 presence of polymeric chitosans and the favoured conditions for oxidation of Pb(II) to Pb(IV) in
302 strongly basic media and its ulterior stabilization. Oxidation of Pb(II) to Pb(IV) turns out to be
303 easier in a strong alkaline medium than in the acidic one (a standard potential of 0.254V – vs.

304 1.460V in acidic media - as can be seen in the Latimer diagram). A similar oxidation, facilitated
305 by the high pH value, has been reported for Co(II)-doped cement systems, in which some
306 Co(III) compounds were identified [51]. The atmospheric oxygen, included during the mixing
307 process, or the abundant Fe(III) ions can be mentioned among the plausible oxidizing agents
308 [51]. According to the HSAB concept, the chemical interaction between a hard base like
309 hydroxyl or oxide anion and a hard acid like Pb(IV) gives rise to a more stable compound than
310 the interaction between the same anions and a softer acid like Pb(II). The chitosan-based
311 polymer, through the hydrophilic characteristics of its functional groups, can retain water giving
312 rise to a gel formation that could facilitate the availability of hydroxyl ions for Pb(IV) ions. In
313 the absence of the hydrophilic polymer, the Pb(IV) was not stabilized , as proved by the fact that
314 Pb(IV) phases were neither identified by XRD nor reported at all.

315 XRD analyses showed chromium to be mainly retained as chromates, since diffraction peaks of
316 $K_2Cr_4O_{13}$ (peak: 25.00º 2θ) and $CaCrO_4$ (24.56º 2θ) were identified. Chromates with different
317 degree of hydration were also found: $CaCrO_4 \cdot 2H_2O$ (20.60º 2θ) in HPCH and MMWCH
318 samples; in HMWCH and MMWCH ($CaCrO_4 \cdot H_2O$; peaks:25.50º, 27.98º 2θ) or in HMWCH
319 ($Ca_9Cr_6O_{24}$; peaks: 30.10º, 33.20º,25.10º 2θ) (Fig. 7c). The occurrence of chromates in samples
320 doped with Cr had also been stated in the literature but in a limited range [40,52]. The XRD
321 study did not allow us to prove the presence of either Cr-ettringite
322 ($3CaO.Al_2O_3 \cdot 3CaCrO_4 \cdot 32H_2O$) or bentorite ($3CaO \cdot Cr_2O_3 \cdot 3CaSO_4 \cdot 32H_2O$), reported by Jain and
323 Garg [40] as the main phases responsible for Cr retention. However, a substitutional compound,
324 resulting from the introduction of Cr(VI) in the calcium silicate net, $CaCr(Si_4O_{10})$ could be
325 identified in MMWCH and LMWCH samples, with diffraction peaks at 23.52º and 29.51º 2θ.
326 By means of XRF, Cr-rich spots were observed and characterized in the studied samples and
327 related to the alkaline chromates found in XRD studies. The mapping (not shown) of the
328 chemical elements carried out by SEM-EDS confirmed that a limited amount of Cr was

329 introduced in the silicate network of the binding phase, since traces of Cr were found in the
330 inter-particles area associated with Ca and Si, and its presence was also checked by XRF.

331

332 3.3. Leaching tests

333 Experimental measurements for every sample showed the same pattern of pH and conductivity,
334 regardless of the heavy metal loaded into the cement (Table 1). The initial pH was around 10,
335 due to the alkaline nature of the S/S matrix, reaching a maximum pH in the fourth fraction, that
336 is, 4 days after the beginning of the leaching test. From this time on, a more or less progressive
337 pH decrease was observed depending on the metal loaded, with a minimum value of pH ca. 9
338 being reached at day 64. A parallel profile was seen for conductivity measurements (Table 1).

339 Fig. 11 shows the log-log cumulative leaching of each one of the metals studied versus time.
340 Heavy metals added as salts were effectively immobilized in the assayed cementitious matrices
341 (99.6% retention for Pb, 99.9% for Zn after 64 days). These data are in good agreement with the
342 results cited by Giergiczny and Król [53]. The maximum cumulative leaching values obtained
343 after 64 days were ca. 58 and 15 $mg.m^{-2}$, for Pb and Zn, respectively, and comply with the limits
344 (400 and 800 $mg.m^{-2}$, for Pb and Zn) imposed by a regulatory norm [54]. The retention
345 observed for Cr was lower (ca. 70-75% after 64 days), again in accordance with the reportedly
346 poor immobilization of this metal [53] and exceeding (4800 $mg.m^{-2}$) the top value (120 $mg.m^{-2}$)
347 indicated in the norm [54]. This distinctive leaching behaviour of Cr vs. Pb and Zn could be
348 explained by means of the knowledge of the different solid-state phases of the metal in the
349 cement samples discussed in the previous section. Whereas Cr tends to be mainly as chromate
350 (CrO_4^{2-}) both Pb and Zn appeared in the hydroxyl form (e.g. $Zn(OH)_4^{2-}$) or as a part of the
351 silicate network, thus enabling the adsorption-immobilization onto the CSH phases.

352 Nearly 80% of the Cr leached was collected in fractions 1 to 3, that is, within the period of time
353 0 to 2.25 days. From the cumulative log-log data evaluation (Fig. 11), a linear regression
354 analysis allowed us to calculate the slopes (with associated standard deviations), which appear
355 in Table 2 [55-57]. A surface washing-off process can take place at the very early stages
356 involving the dissolution of the most of the soluble material on the surface. This process would
357 typically result in a slope < 0.35 [58,59]. In samples HMWCH and HPCH, an initial surface
358 washing process can not totally be ruled out because the slope values, considering the standard
359 deviation, ranged from 0.325 to 0.477 (HMWCH) and from 0.292 to 0.434 (HPCH), thus in
360 some cases falling below 0.35 (time increment 1-4 in Table 2). This was also supported by the
361 most important release of chromium that took place at the first leaching stages [56,60]. Given
362 that the values of the slopes also appeared within the range of a diffusion-controlled mechanism
363 (between 0.35 and 0.65), the leaching behaviour of chromium in samples HMWCH and HPCH
364 at early stages can be explained by a combination of both surface wash-off and diffusion
365 processes, with depletion occurring later. As for polymer free, LMWCH and MMWCH Cr-
366 doped samples, a slope close to 0.5 was found suggesting that the main governing leaching
367 mechanism was diffusion at early stages [61], followed by depletion at later stages [55],
368 according to the interpretation of the EA NEN 7375:2004 [37], also described by Lampris et al.
369 [62] and Ginés et al. [56]. The pH values in the first step of the leaching test (6 hours) for these
370 Cr-bearing samples were the lowest. This fact can be ascribed to the release of chromates and
371 their subsequent hydrolysis which forces a pH decrease. After near complete depletion of Cr
372 (Fig. 11a), that took place between the second and third step of the leaching test, the pH
373 increased owing to the hydration of the calcium silicates and the portlandite formation.

374 Largest concentration of Pb was measured in the first fraction and the leaching continued up to
375 day 9. Highest pH values were reached in the first leaching step because the released Pb
376 compounds did not show acidic hydrolysis, especially when compared with Cr compounds. The

377 great porosity induced by the addition of LMWCH to the mortar is in good accordance with the
378 higher values of lead found in the LMWCH-modified cement leachates. As deducible from the
379 slopes summarized in Table 2, the leaching occurred through (i) a controlled diffusion (slope
380 values between 0.35 and 0.65) or delayed diffusion mechanism (slope > 0.65) at early stages
381 and (ii) a depletion mechanism at later steps (slope < 0.35). In general, the controlled-diffusion
382 mechanism spanned 9 days (time increment 2-5 in Table 2), which is coherent with the better
383 retention of Pb as compared with Cr.

384 The Zn-loaded HPCH mortars yielded the highest values of conductivity and pH, what is an
385 indication of the largest quantity of Zn leached (Fig. 11c). On the other hand, the LMWCH
386 sample exhibited the lowest conductivity of all Zn-loaded polymer-modified samples, and –
387 subsequently- showed the lowest values of leached Zn.

388 The calculated slopes reported in Table 2 show a delayed diffusion-controlled mechanism as a
389 consequence of the better chemical immobilization of Zn which results in a sluggish leaching
390 (dissolution mechanism) up to fraction 5 (time increment 2-5) (slope > 0.65) . This mechanism
391 is also supported by the low leaching values achieved for Zn despite of the large porosity of the
392 mortars (see, for example, the large porosity of polymer-free mortar in Fig. 6 while retaining a
393 large ratio of Zn). Therefore, in the overall release of Zn, permeability plays, if any, a minor
394 role, the chemical fixation accounting for most of the metal retention rather than a physical
395 entrapment. Such hypothesis had been claimed before [46] and it is now here confirmed. The
396 improvement observed in the retention of Zn in the LMWCH-mortars (by 24% with respect to
397 the polymer-free mortars) can be directly linked to the above discussed formation of dietrichite
398 that confers the chemical stabilization of this metal in the cement matrix. This fact, together
399 with the rise in the mechanical strength of the mortar, emphasizes the usefulness of chitosan in
400 S/S process of Zn in cement mortars.

The rate of leaching of these metals was estimated by the value of the negative logarithm of the effective diffusion coefficient, according to the assessment of a diffusion coefficient in the EA NEN 7375:2004 norm, also described in previous works [7,63,64]. The calculated pDe global value for Cr was 12.5 (De= $3.16 \cdot 10^{-13}$ $m^2 \cdot s^{-1}$), on the border line between low and average mobility. These findings support the shorter period of the diffusion mechanism and the higher concentration of Cr in the leachates. Both Pb and Zn showed, in general, pDe values higher than 13.1 (De > $7.94 \cdot 10^{-14}$ $m^2 \cdot s^{-1}$), allowing us to classify them as low mobility metals. These experimental results of the effective diffusion coefficient are in good agreement with a previous work reporting De values of the studied heavy metals in cement materials [64,65], confirming the chemical interaction between the metals and the hydration products of cement.

4. Conclusions

Characterization studies led to the identification of newly reported compounds for the retention of the three studied toxic metals, Cr, Pb and Zn.

In the presence of LMWCH, Zn was mainly retained as dietrichite ($ZnAl_2(SO_4)_4.22H_2O$). In the presence of other chitosan polymers as well as in the free-polymer mortar, calcium hydroxozincate was identified. These chemical phases are held responsible for the retention of Zn in lieu of the substitutional compounds in the silicate network. The presence of these phases justified the dramatic changes undergone in the fresh and hardened state properties of cement mortars upon addition of Zn.

All the assayed polymers, native and etherified chitosans, improved the characteristics of the hardened Zn-bearing mortars, notably enhancing the compressive strength as a consequence of the total reduction in porosity. Leaching tests showed that the incorporation of LMWCH had a beneficial effect retaining Zn in a much larger ratio (24% increase with respect to the polymer

free mortar) as a consequence of its chemical fixation as dietrichite. A diffusion-controlled release was evidenced for this metal and permeability was proved to play only a secondary role.

For the first time Pb-bearing silicates (i.e. plumalsite, $Pb_4Al_2(SiO_3)_7$, lead silicate hydrate, $Pb_2SiO_4 \cdot xH_2O$, and alamosite, $PbSiO_3$) were identified by XRD, confirming that Pb was mainly retained as a part of the silicate network after Ca ion exchange. The presence and the subsequent action of the polymers also favoured the formation and stabilization of new Pb(IV) forms, characterized as K_4PbO_4, Ca_2PbO_4 and PbO_2. High retention values (99.6%) for Pb were explained in terms of its chemical solidification/stabilization.

An ample variety of both anhydrous and hydrated chromate species were identified for Cr(VI) retention ($K_2Cr_4O_{13}$, $CaCrO_4$, $CaCrO_4 \cdot 2H_2O$, $CaCrO_4 \cdot H_2O$, $Ca_9Cr_6O_{24}$). Contrary to the observed behaviour for Pb and Zn, leaching of chromium was facilitated from these species in the hardened cement matrix.

The addition of the toxic metals to the cement mortars modified to a large extent the setting times, but, in general, the incorporation of the natural polymers lessened the detrimental effects of the toxic metals, improving the handling of mortars. This finding is interesting from a technological point of view in S/S processes.

In the research field of toxic metal immobilization in cement mortars, this work shows a possible trend in order to use polymers for improving cement mortars characteristics and/or toxic metal encapsulation.

Acknowledgements

This work was funded by the Ministry of Science of Spain (MAT2007-65478) and Fundación Universitaria de Navarra (FUNA2010-15108152). M. Lasheras-Zubiate thanks the Friends of the University of Navarra, Inc., for funding support.

References

[1] X.C. Qiao, C.S. Poon, C.R. Cheeseman, Transfer mechanisms if contaminants in cement-based stabilized/solidified wastes, J Hazard Mater 129 (2006), pp. 290-296.

[2] C.Y. Yin, H.B. Mahmudb, M.G. Shaaban, Stabilization/solidification of lead-contaminated soil using cement and rice husk ash, J Hazard Mater 137 (2006), pp.1758-1764.

[3] M.A.C. Gollmann, M.M. da Silva, A.B. Masuero, J.H.Z. dos Santos, Stabilization and solidification of Pb in cement matrices, J Hazard Mater 179 (2010), pp. 507-514.

[4] M.I. Ojovan, G.A. Varlackova, Z.I. Golubeva, O.N. Burlaka, Long-term field and laboratory leaching tests of cemented radioactive wastes, J Hazard Mater 187 (2011), pp. 296-302

[5] X.D. Li, C.S. Poon, H. Sun, M.C. Lo, D.W. Kirk, Heavy metal speciation and leaching behaviors in cement based solidified/stabilized waste materials, J Hazard Mater 82 (2001), pp. 215-230.

[6] J.R. Conner, S.L. Hoeffner, A critical review of stabilization/solidification technology, Environ Sci Technol 28 (1998), pp. 397-462.

[7] R. Malviya, R. Chaudhary, Leaching behaviour and immobilization of heavy metals in solidified/stabilizaed products, J Hazard Mater 137 (2006), pp. 207-217.

[8] L. Zampori, I. Natali Sora, R. Pelosato, G. Dotelli, P.G. Gallo Stampino, Chemistry of cement hydration in polymer-modified pastes containing lead compounds, J Eur Ceram Soc 26 (2006), pp. 809-816.

[9] V.A. Rossetti, F. Medici, Inertization of toxic metals in cement matrices: Effects on hydration, setting and hardening, Cem Concr Res 25 (1996), pp. 1147-1152.

[10] C.K. Park, Hydration and solidification of hazardous wastes containing heavy metals using modified cementitious materials, Cem Concr Res 30 (2000), pp. 429-435.

[11] N. Gineys, G. Aouad, D. Damidot, Managing trace elements in Portland cement – Part I: Interactions between cement paste and heavy metals added during mixing as soluble salts, Cem Concr Compos 32 (2010), pp. 563-570.

476 [12] S. Berger, C. Cau Dit Coumes, P. Le Bescop, D. Damidot, Hydration of calcium
477 sulfoaluminate cement by a $ZnCl_2$ solution: Investigation at early age, Cem Concr Res
478 39 (2009), pp. 1180-1187.
479 [13] L. Zhang, L.J.J. Catalan, A.C. Larsen, S.D. Kinrade, Effects of sucrose and sorbitol on
480 cement-based stabilization/solidification of toxic metal waste, J Hazard Mater 151
481 (2008), pp. 490-498.
482 [14] D.L. Cocke, The binding chemistry and leaching mechanisms of hazardous substances in
483 cementitious solidification/stabilization systems. J Hazard Mater 24 (1990), pp. 231-253.
484 [15] C. Tashiro, Hardening property of cement mortar adding heavy metal compound and
485 solubility of heavy metal from hardened mortar, Cem Concr Res 7 (1977), pp. 283-290.
486 [16] O.E. Omotoso, D.G. Ivey, R. Mikula, Hexavalent chromium in tricalcium silicate. J Mater
487 Sci 33 (1998), pp. 507-513.
488 [17] S. Bagosi, L.J. Csetenyi, Immobilization of caesium-loaded ion exchange resins in zeolite-
489 cement blends, Cem Concr Res 29 (1999), pp. 479-485.
490 [18] M.A. Tantawy, A.M. El-Roudi, A.A. Salem, Immobilization of Cr(VI) in bagasse ash
491 blended cement pastes, Constr Build Mater 30 (2012), pp. 218-223.
492 [19] W. Mozgawa, M. Król, W. Pichór, Use of clinoptilolite for the immobilization of heavy
493 metal ions and preparation of autoclaved building composites, J Hazard Mater 168
494 (2009), pp. 1482-1489.
495 [20] G.E. Voglar, D. Leštan, Efficiency modeling of solidification/stabilization of multi-metal
496 contaminated industrial soil using cement and additives, J Hazard Mater 192 (2011), pp.
497 753-762.
498 [21] H.S. Shi, L.L. Kan, Study on the properties of chromium residue-cement matrices (CRCM)
499 and the influences of superplasticizers on chromium(VI)-immobilising capability of
500 cement matrices, J Hazard Mater 162 (2009), pp. 913-919.
501 [22] P. Gallo Stampino, L. Zampori, G. Dotelli, P. Meloni, I. Natali Sora, R. Pelosato, Use of
502 admixtures in organic-contaminated cement–clay pastes, J Hazard Mater 161 (2009), pp.
503 862-870
504 [23] M. Lasheras-Zubiate, I. Navarro-Blasco, J.M. Fernández, J.I. Álvarez, Studies on chitosan
505 as an admixture for cement-based materials: assessment of its viscosity enhancing effect
506 and complexing ability for heavy metals. J Appl Polym Sci 120 (2011), pp. 242-252.
507 [24] M. Lasheras-Zubiate, I. Navarro-Blasco, J.I. Álvarez, J.M. Fernández, Interaction of
508 carboxymethylchitosan and heavy metals in cement media. J Hazard Mater 194 (2011),
509 pp. 223-231.

510 [25] International Patent, 2012. Use of carboxymethyl chitosans as additives in agglomerating
511 compositions. n° WO/2012/042090.
512 [26] M. Lasheras-Zubiate, I. Navarro-Blasco, J.M. Fernández, J.I. Álvarez, Effect of the
513 addition of chitosan ethers on the fresh state properties of cement mortars, Cem Concr
514 Compos (2012), doi: 10.1016/j.cemconcomp.2012.04.010.
515 [27] G. Laforest, J. Duchesne. Stabilization of electric arc furnance dust by the use of
516 cementitious materials: Ionic competition and long-term stability. Cem Concr Res 36
517 (2006), pp. 1628-1634.
518 [28] S. Peysson, J. Péra, M. Chabannet, Immobillization of heavy metals by calcium
519 sulfoaluminate cement. Cem Concr Res 35 (2005), pp. 2261-2270.
520 [29] O. Yamaguchi, M. Ida, Y. Uchiyama, S. Hanehara, A method for the determination of total
521 Cr(VI) in cement. J Eur Ceram Soc 26 (2006), pp. 785-790.
522 [30] Y. Peng, B. Han, W. Liu, X. Xu, Preparation and antimicrobial activity of hydroxypropyl
523 chitosan. Carbohydr Res 340 (2005), pp. 1846-1851.
524 [31] A. Izaguirre, J. Lanas, J.I. Álvarez, Effect of water-repellent admixtures on the behaviour
525 of aerial lime-based mortars. Cem Concr Res 39 (2009), pp. 1095-1104.
526 [32] N.L. Thomas, D.A. Jameson, D.D. Couble, The effect of lead nitrate on the early hydration
527 of Portland cement. Cem Concr Res 11 (1981), pp. 143-153.
528 [33] EN 1015-2 Methods of test for mortar for masonry - Bulk sampling of mortars and
529 preparation of test mortars. 1999.
530 [34] EN 1015-3 Methods of test mortar for masonry. Part 3: Determination of consistence of
531 fresh mortar (by flow table). 2000.
532 [35] UNE 83-818 Test methods. Mortars. Fresh mortars. Determination of water retentivity.
533 1993.
534 [36] EN 1015-9 Methods of test mortar for masonry. Part 9: Determination of workable life and
535 correction time of fresh mortar. 2000.
536 [37] EA NEN 7375 Leaching characteristics of moulded or monolithic building and waste
537 materials. Determination of leaching of inorganic components with the diffusion test.
538 2004.
539 [38] C. Weeks, R.J. Hand, J.H. Sharp, Retardation of cement hydration caused by heavy metals
540 present in ISF slag used as aggregate. Cem Concr Compos 30 (2008), pp. 970-978.
541 [39] J.N. Diet, P. Moszkowicz, D. Sorrentino, Behaviour of ordinary Portland cement during the
542 stabilization/solidification of synthetic heavy metal sludge: macroscopic and
543 microscopic aspects, Waste Manage. 18 (1998), pp. 17-24.

544 [40] N. Jain, M. Garg, Effect of Cr(VI) on the hydration behavior of marble dust blended
545 cement: Solidification, leachability and XRD analyses, Constr. Build. Mater. 22 (2008),
546 pp. 1851-1856.
547 [41] M.A. Trezza, M.F. Ferraiuelo, Hydration study of limestone blended cement in the
548 presence of hazardous wastes containing Cr(VI), Cem Concr Res. 33 (2003), pp. 1039-
549 1045.
550 [42] R. Malviya, R. Chaudhary, Factors affecting hazardous waste solidification/stabilization: A
551 review. J Hazard Mater 137 (2006), pp. 267–276.
552 [43] US EPA 625/6–89/022, Stabilization/Solidification of CERCLA and RCRA Wastes –
553 Physical Tests, Chemical Testing Procedures, Technology Screening, and Field
554 Activities. 1989.
555 [44] B. Pandey, S.D. Kinrade, L.J.J. Catalan, Effects of carbonation on the leachability and
556 compressive strength of cement-solidified and geopolymer-solidified synthetic metal
557 wastes, J Environ Manage 101 (2012), pp. 59-67.
558 [45] I. Fernández Olmo, E. Chacón, A. Irabien, Influence of lead, zinc, iron (III) and chromium
559 (III) oxides on the setting time and strength development of Portland cement. Cem
560 Concr Res 31 (2001), pp. 1213-1219.
561 [46] C.S. Poon, C.J. Peters, R. Perry, P. Barnes, A.P. Barker, Mechanisms of metal stabilization
562 by cement based fixation processes, Sci. Total Environ. 41 (1985), pp. 55-71.
563 [47] A. Zingg, F. Winnefeld, L. Holzer, J. Pakusch, S. Becker, R. Figi, L. Gauckler, Interaction
564 of polycarboxylate-based superplasticizers with cements containing different C3A
565 amounts, Cem. Concr. Compos. 31 (2009), pp. 153-162.
566 [48] D. Lee, Formation of leadhillite and calcium lead silicate hydrate (C-Pb-S-H) in the
567 solidification/stabilization of lead contaminants, Chemosphere 66 (2007), pp. 1727-
568 1733.
569 [49] H. Yoo, D. Lee, The microstructure of Pb-doped solidified waste forms using Portland
570 cement and calcite, Environ. Eng. Res. 11 (2006), pp. 54-61.
571 [50] Q.Y. Chen, C.D. Hills, M. Tyrer, I. Slipper, H.G. Shen, A. Brough, Characterisation of
572 products of tricalcium silicate hydration in the presence of heavy metals, J. Hazard. Mat.
573 147 (2007), pp. 817-825.
574 [51] M. Vespa, R. Dähn, D. Grolimund, M. Harfouche, E. Wieland, A.M. Scheidegger,
575 Speciation of heavy metals in cement-stabilized waste forms: A micro-spectroscopic
576 study, J. Geochem. Explor. 88 (2006), pp. 77-80.

577 [52] S. Wang, C. Vipulanandan, Solidification/stabilization of Cr(VI) with cement. Leachability
578 and XRD analyses, Cem. Concr. Res. 30 (2000), pp. 385-389.
579 [53] Z. Giergiczny, A. Król, Immobilization of heavy metals (Pb, Cu, Cr, Zn, Cd, Mn) in the
580 mineral additions containing concrete composites, J. Hazard. Mat. 160 (2008), pp. 247-
581 255.
582 [54] Dutch Soil Quality Regulation, 10 October 2006.
583 [55] C. Lampris, J.A. Stegemann, C.R. Cheeseman, Chloride leaching from air pollution control
584 residues solidified using ground granulated blast furnace slag, Chemosphere, 73 (2008),
585 pp.1544-1549.
586 [56] O. Ginés, J.M. Chimenos, A. Vizcarro, J. Formosa, J.R. Rosell, Combined use of MSWI
587 bottom ash and fly ash as aggregate in concrete formulation: Environmental and
588 mechanical considerations, J. Hazard. Mat. 169 (2009), pp. 643-650
589 [57] R. Piyapanuwat, S. Asavapisit, Performance of lime-BHA solidified plating sludge in the
590 presence of Na2SiO3 and Na2CO3, J. Environ. Manage. 92 (2011), pp. 2222-2228
591 [58] D.H. Moon, D. Dermatas, An evaluation of lead leachability from stabilized/solidified soils
592 under modified semi-dynamic leaching conditions, Eng. Geol., 85 (2006), Pages 67-74
593 [59] R.O. Abdel Rahman, A.A. Zaki, Assessment of the leaching characteristics of incineration
594 ashes in cement matrix, Chem. Eng. J., 155 (2009), pp. 698-708
595 [60] R.O. Abdel Rahman, A.A. Zaki, A.M. El-Kamash, Modeling the long-term leaching
596 behavior of 137Cs, 60Co, and 152,154Eu radionuclides from cement–clay matrices, J.
597 Hazard. Mat., 145 (2007), pp. 372-380
598 [61] C. Bobirica, L. Bobirica, R. Stanescu, I. Constantinescu, Leaching behavior of cement-
599 based solidified wastes containing hexavalent chromium. UPB Sci. Bull. 72 (2010), pp.:
600 122-128.
601 [62] C. Lampris, J.A. Stegemann, M. Pellizon-Birelli, G.D. Fowler, C.R. Cheeseman, Metal
602 leaching from monolithic stabilised/solidified air pollution control residues, J. Hazard.
603 Mat., 185 (2011), pp. 1115-1123
604 [63] R.Shirley, L. Black, Alkali activated solidification/stabilisation of air pollution control
605 residues and co-fired pulverised fuel ash, J. Hazard. Mat., 194 (2011), pp. 232-242
606 [64] Y. Yang, Q. Huang, Y. Yang, Z. Huang, Q. Wang, Formulation of criteria for pollution
607 control on cement products produced from solid wastes in China, J. Environ. Manage.,
608 92 (2011), pp. 1931-1937.

609 [65] Z. Cai, Dirch H. Bager, T.H. Christensen, Leaching from solid waste incineration ashes
610 used in cement-treated base layers for pavements, Waste Manage., 24 (2004), pp. 603-
611 612.
612
613
614
615
616

617 FIGURE CAPTIONS

618

619 **Figure 1.** Basic structures of chitosan and the etherified derivative (HPCH).

620 **Figure 2**. Effect of the addition of different chitosan-based polymers on the slump values of
621 fresh cement mortars without metal and loaded with either Cr or Pb. Zn values could not be
622 determined because of the disaggregation of the sample.

623 **Figure 3.** Effect of the addition of different chitosan-based polymers on the water retention
624 ability of fresh cement mortars without metal and loaded with Cr, Pb and Zn.

625 **Figure 4**. Influence of the chitosan-based polymer addition on the setting time of fresh cement
626 mortars without metals and loaded with either Cr or Pb. Zn values could not be determined
627 because of the disaggregation of the sample.

628 **Figure 5**. Effect of the addition of different chitosan-based polymers on the compressive
629 strength of cement mortars without metal and loaded with Cr, Pb and Zn.

630 **Figure 6**. Pore size distribution of cement mortars modified by chitosan-based polymers in
631 presence of: (a) Cr, (b) Pb, (c) Zn.

632 **Figure 7.** XRD-identified crystalline phases: a) Zn-; b) Pb-; and c) Cr-bearing mortars.

633 **Figure 8.** Example of Zn-loaded cement mortar (HMWCH) and X-ray mapping of Zn, Ca, Al
634 and Fe. In the colored SEM image, red areas (brighter areas in black/white images) are related
635 to Si-compounds (specially siliceous particles of the aggregate) that appear embedded in the
636 binding matrix. The X-ray mapping images show that Zn is mainly associated to Ca, Al and Fe-
637 bearing phases.

638 **Figure 9.** X-ray fluorescence spectrum of a Zn-rich spot in a chitosan-modified sample,
639 showing Zn associated to calcium and iron phases. Silicon is present to a much lesser extent.

640 **Figure 10**. Pb-loaded cement mortar modified by LMWCH and X-ray mapping of Pb, Ca and
641 Si. In the colored SEM image: brightest and red areas are Si-rich phases from the aggregate,
642 embedded in the binding material, with blue points representing calcium. Distinct green points
643 denote the presence of lead in the binding matrix.

644 **Figure 11.** Log of cumulative leaching versus log of time for (a)Cr, (b) Pb and (c)Zn over 64
645 days.

Table 1

Table 1. Values of pH and electrical conductivity (EC) (µS cm^{-1}) of the respective leachates of Cr, Pb and Zn-bearing mortars over the eight steps of the leaching test.

Cr																
Step of leaching test	1		2		3		4		5		6		7		8	
	pH	EC	pH	EC	pH	EC	pH	EC	pH	EC	pH	EC	pH	EC	pH	EC
Polymer free	9.87	132.8	10.52	171.7	11.04	225.9	11.15	150.2	10.70	146.5	9.41	88.6	8.78	80.4	8.54	83.8
LMWCH	9.83	135.7	10.43	203.0	10.88	268.6	11.58	202.1	10.98	183.9	10.05	113.7	8.65	80.9	8.56	79.6
MMWCH	9.52	170.2	10.13	196.1	10.82	195.0	10.95	213.3	10.81	228.5	10.10	146.0	8.77	83.5	8.74	96.5
HMWCH	9.88	153.9	10.96	245.9	10.60	225.9	10.79	187.0	10.73	197.5	9.74	98.8	8.93	81.9	8.63	78.3
HPCH	10.19	259.7	10.55	236.7	10.53	228.9	10.69	190.0	10.40	153.9	8.92	99.3	8.93	78.4	8.69	81.1
Pb																
Step of leaching test	1		2		3		4		5		6		7		8	
	pH	EC	pH	EC	pH	EC	pH	EC	pH	EC	pH	EC	pH	EC	pH	EC
Polymer free	10.79	274.9	10.91	331.0	11.21	278.4	11.10	298.0	10.40	137.8	9.62	97.2	8.75	90.2	8.48	101.9
LMWCH	11.06	450.0	11.11	531.0	11.45	418.0	11.10	291.3	10.21	161.0	9.63	81.7	8.87	87.8	8.49	104.6
MMWCH	11.07	348.0	11.38	412.0	10.97	327.0	11.11	300.0	11.00	276.5	10.05	112.2	9.11	83.7	8.39	102.1
HMWCH	11.07	443.0	11.11	534.0	11.28	366.0	11.11	289.4	10.72	220.7	9.17	93.6	9.17	83.3	8.70	95.6
HPCH	11.02	400.0	11.04	445.0	11.23	445.0	11.17	292.3	10.42	127.4	9.56	87.5	8.79	89.0	8.59	94.4
Zn																
Step of leaching test	1		2		3		4		5		6		7		8	
	pH	EC	pH	EC	pH	EC	pH	EC	pH	EC	pH	EC	pH	EC	pH	EC
Polymer free	9.89	197.8	8.67	162.2	10.56	252.3	11.42	186.5	11.26	356.0	10.46	210.4	9.30	107.0	8.85	115.8
LMWCH	9.83	208.8	10.31	159.5	10.64	218.6	11.03	200.4	10.94	188.3	10.29	203.0	9.79	121.2	9.13	105.4
MMWCH	10.12	212.3	10.47	231.5	10.52	193.9	10.92	251.9	10.94	311.0	10.52	255.6	9.17	100.8	9.04	117.5
HMWCH	10.16	197.2	10.55	242.0	11.05	241.9	11.12	319.0	10.75	368.0	10.59	210.4	9.27	90.3	8.95	107.9
HPCH	10.31	223.4	10.68	308.0	11.24	398.0	11.17	419.0	10.91	492.0	11.16	556.0	10.49	247.3	9.22	139.7

Table 2. Calculated slopes and associated standard deviation of the log–log plots of derived cumulative leaching vs. time for different time increments (Increment 1-4: from 0.25 to 4 days; Increment 2-5: from 1 to 9 days; Increment 3-6: from 2.25 to 16 days; Increment 4-7: from 4 to 36 days; Increment 5-8: from 9 to 64 days).

Cr					
Step	***Polymer free***	***LMWCH***	***MMWCH***	***HMWCH***	***HPCH***
Increment 1-4	0.444±0.077	0.557±0.103	0.472±0.077	0.401±0.076	0.363±0.071
Increment 2-5	0.183±0.034	0.199±0.058	0.220±0.028	0.159±0.026	0.131±0.028
Increment 3-6	0.115±0.015	0.083±0.013	0.160±0.019	0.115±0.008	0.073±0.011
Increment 4-7	0.088±0.003	0.056±0.003	0.121±0.005	0.098±0.006	0.053±0.001
Increment 5-8	0.092±0.004	0.055±0.003	0.114±0.002	0.092±0.008	0.057±0.004
Pb					
Step	***Polymer free***	***LMWCH***	***MMWCH***	***HMWCH***	***HPCH***
Increment 1-4	0.382±0.027	0.561±0.031	0.812±0.041	0.630±0.032	0.546±0.037
Increment 2-5	0.234±0.046	0.375±0.058	0.616±0.166	0.437±0.060	0.316±0.074
Increment 3-6	0.112±0.035	0.235±0.160	0.252±0.139	0.255±0.075	0.187±0.057
Increment 4-7	0.132±0.042	0.087±0.030	0.014±0.008	0.080±0.043	0.097±0.013
Increment 5-8	0.143±0.042	0.024±0.014	0.001±0.001	0.002±0.001	0.081±0.022
Zn					
Step	***Polymer free***	***LMWCH***	***MMWCH***	***HMWCH***	***HPCH***
Increment 1-4	0.741±0.179	0.727±0.006	0.718±0.104	0.819±0.061	0.649±0.066
Increment 2-5	1.016±0.109	0.804±0.044	0.822±0.101	0.865±0.067	0.689±0.074
Increment 3-6	0.595±0.199	0.631±0.151	0.454±0.114	0.565±0.116	0.368±0.116
Increment 4-7	0.164±0.127	0.287±0.185	0.200±0.135	0.272±0.159	0.090±0.123
Increment 5-8	0.044±0.024	0.031±0.019	0.034±0.017	0.015±0.002	0.108±0.019

Figure 1

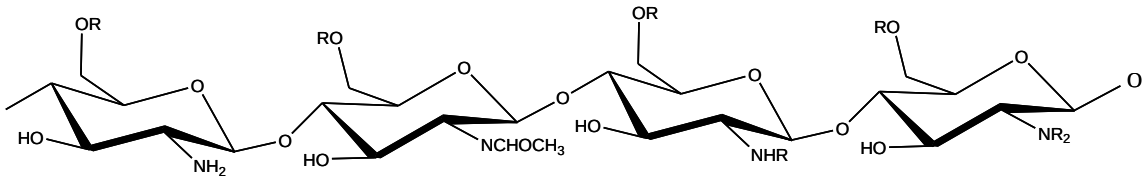

For native chitosan: R = -H

For HPCH derivative: R = -H, $-(CH_2)_3OH$

Figure 1. Basic structures of chitosan and the etherified derivative (HPCH).

Figure 2

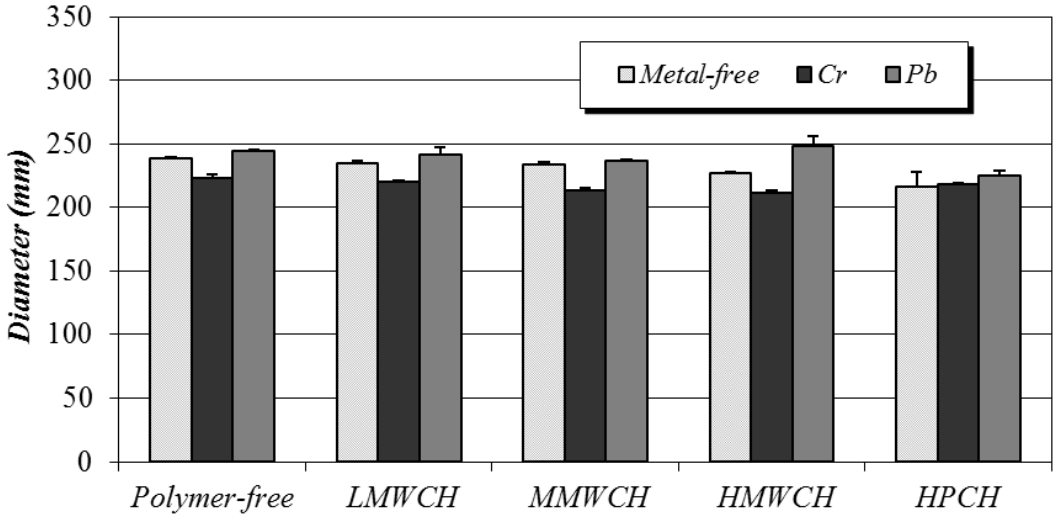

Figure 2. Effect of the addition of different chitosan-based polymers on the slump values of fresh cement mortars without metal and loaded with either Cr or Pb. Zn values could not be determined because of the disaggregation of the sample.

Figure 3

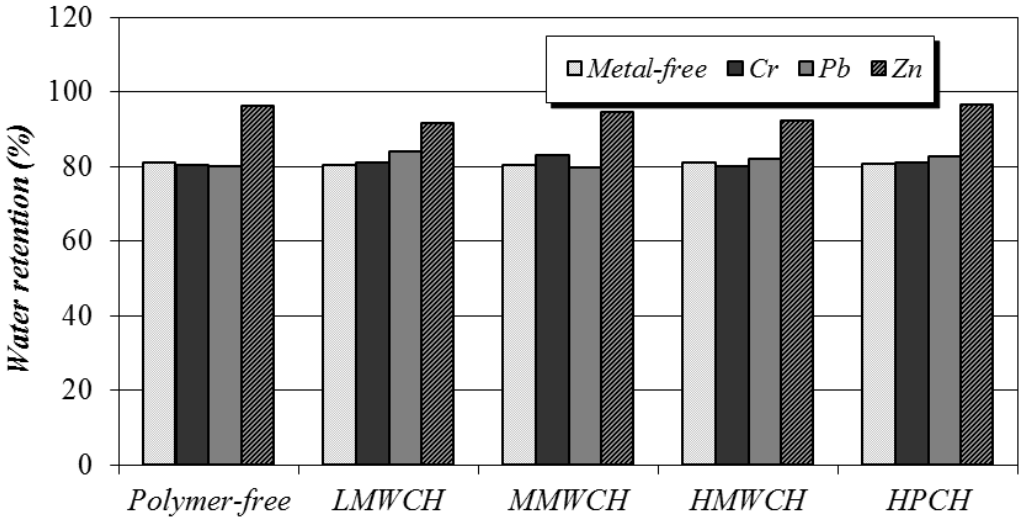

Figure 3. Effect of the addition of different chitosan-based polymers on the water retention ability of fresh cement mortars without metal and loaded with Cr, Pb and Zn.

Figure 4

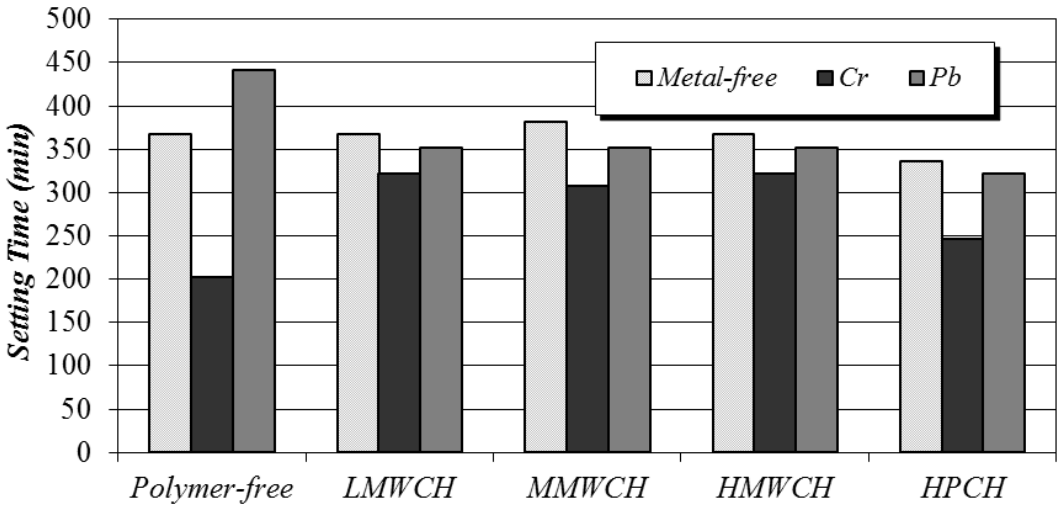

Figure 4. Influence of the chitosan-based polymer addition on the setting time fresh cement mortars without metals and loaded with either Cr or Pb. Zn values could not be determined because of the disaggregation of the sample.

Figure 5

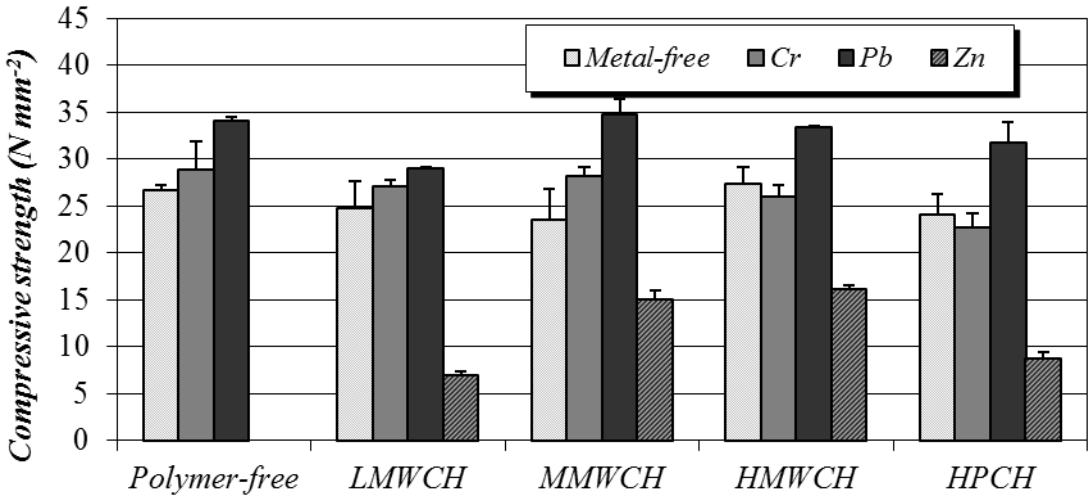

Figure 5. Effect of the addition of different chitosan-based polymers on the compressive strength of cement mortars without metal and loaded with Cr, Pb and Zn.

Figure 6

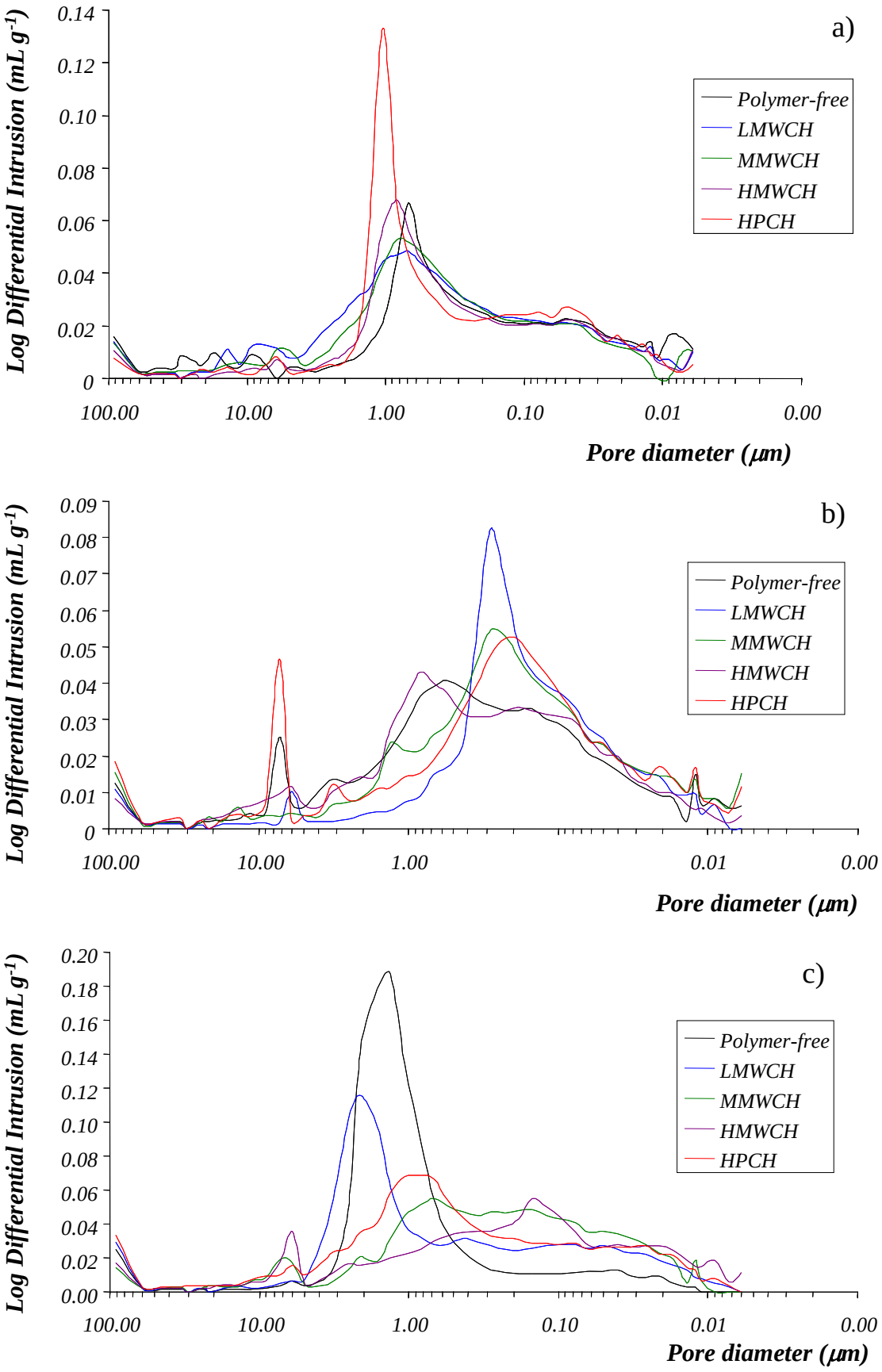

Figure 6. Pore size distribution of cement mortars modified by chitosan-based polymers in presence of: (a) Cr, (b) Pb, (c) Zn.

Figure 7

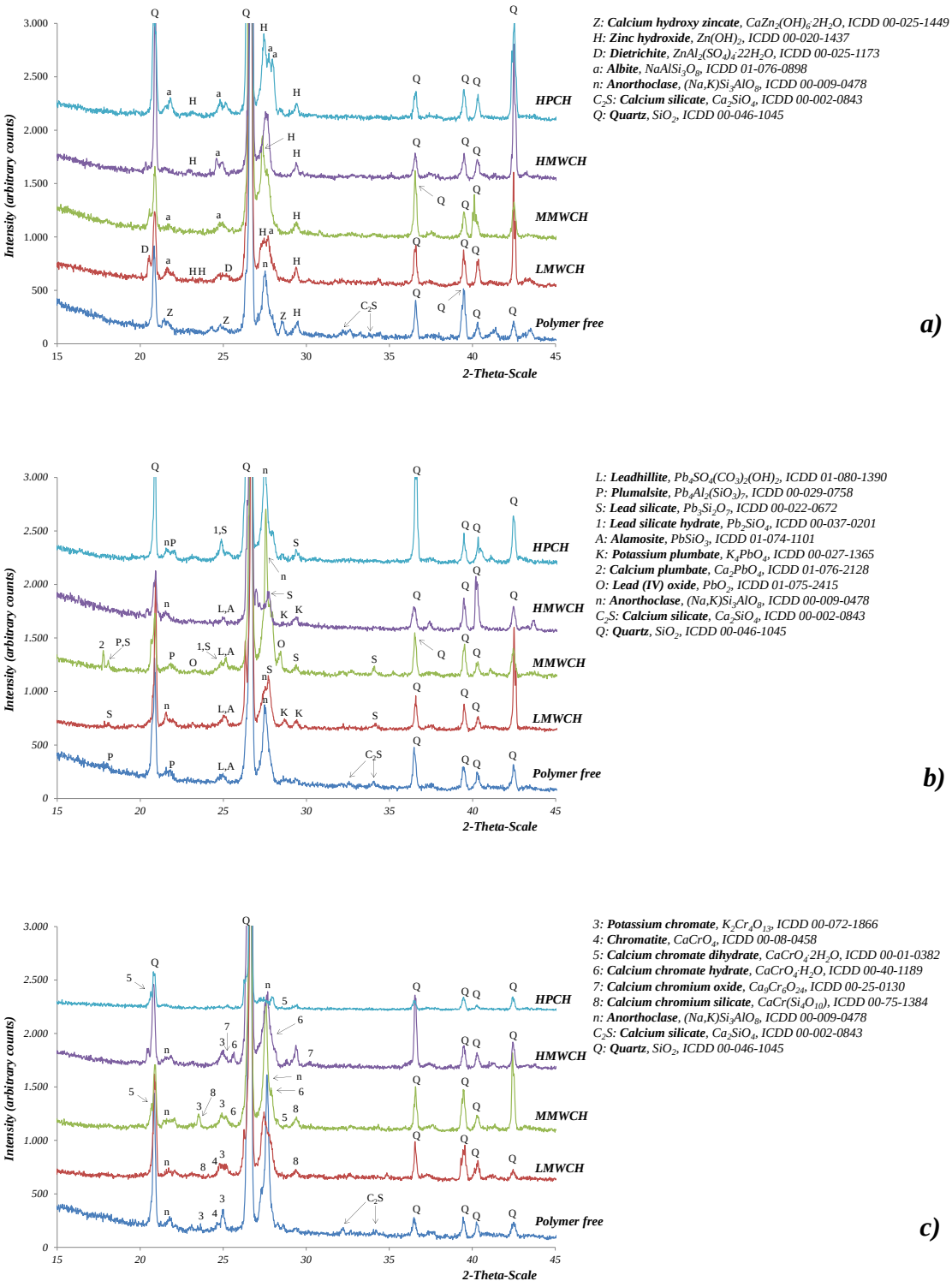

Figure 7. XRD-identified crystalline phases: a) Zn-; b) Pb-; and c) Cr-bearing mortars.

Figure 8

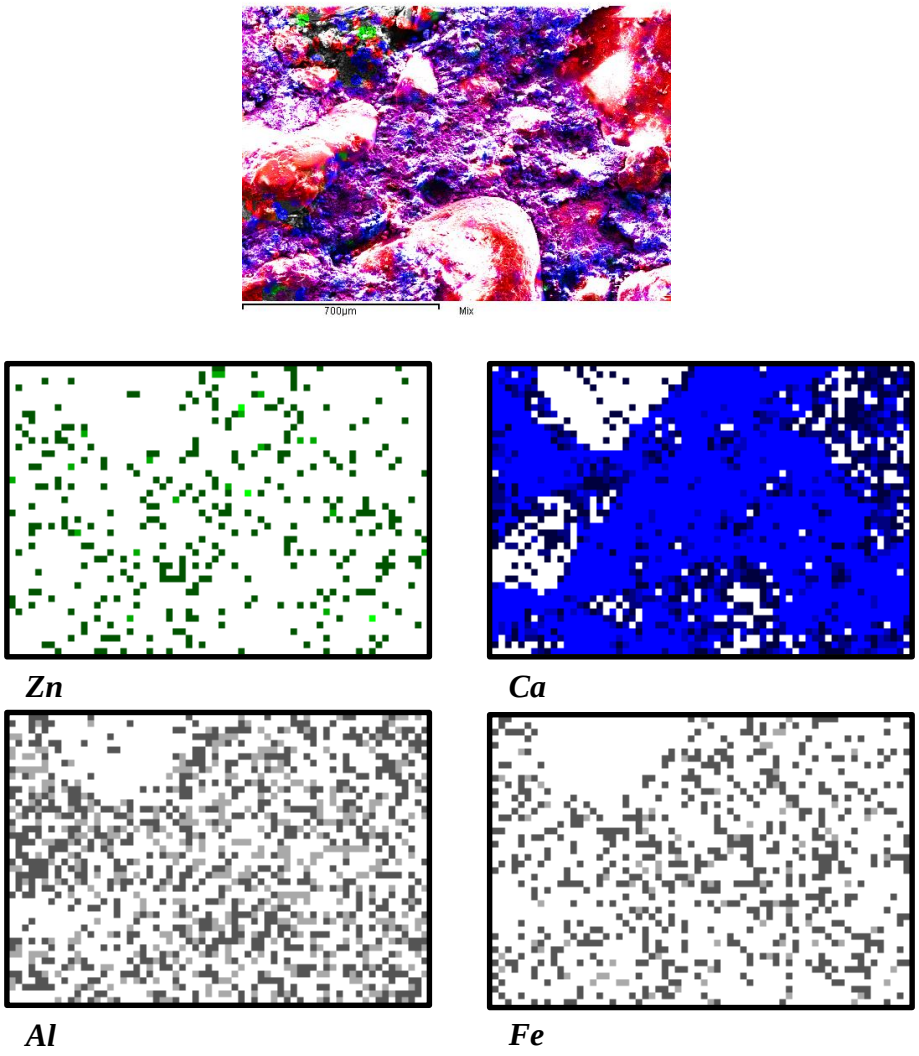

Figure 8. Example of Zn-loaded cement mortar (HMWCH) and X-ray mapping of Zn, Ca, Al and Fe. In the colored SEM image, red areas (brighter areas in black/white images) are related to Si-compounds (specially siliceous particles of the aggregate) that appear embedded in the binding matrix. The X-ray mapping images show that Zn is mainly associated to Ca, Al and Fe-bearing phases.

Figure 9

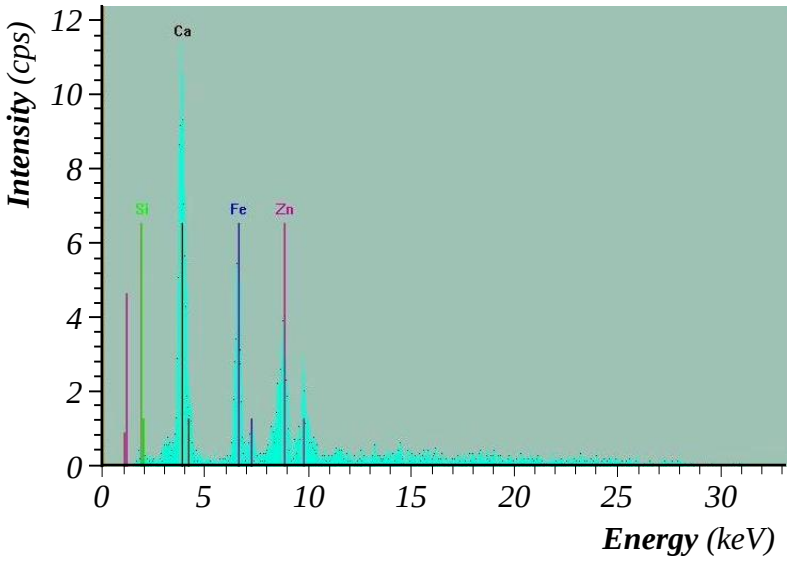

Figure 9. X-ray fluorescence spectrum of a Zn-rich spot in a chitosan-modified sample, showing Zn associated to calcium and iron phases. Silicon is present to a much lesser extent.

Figure 10

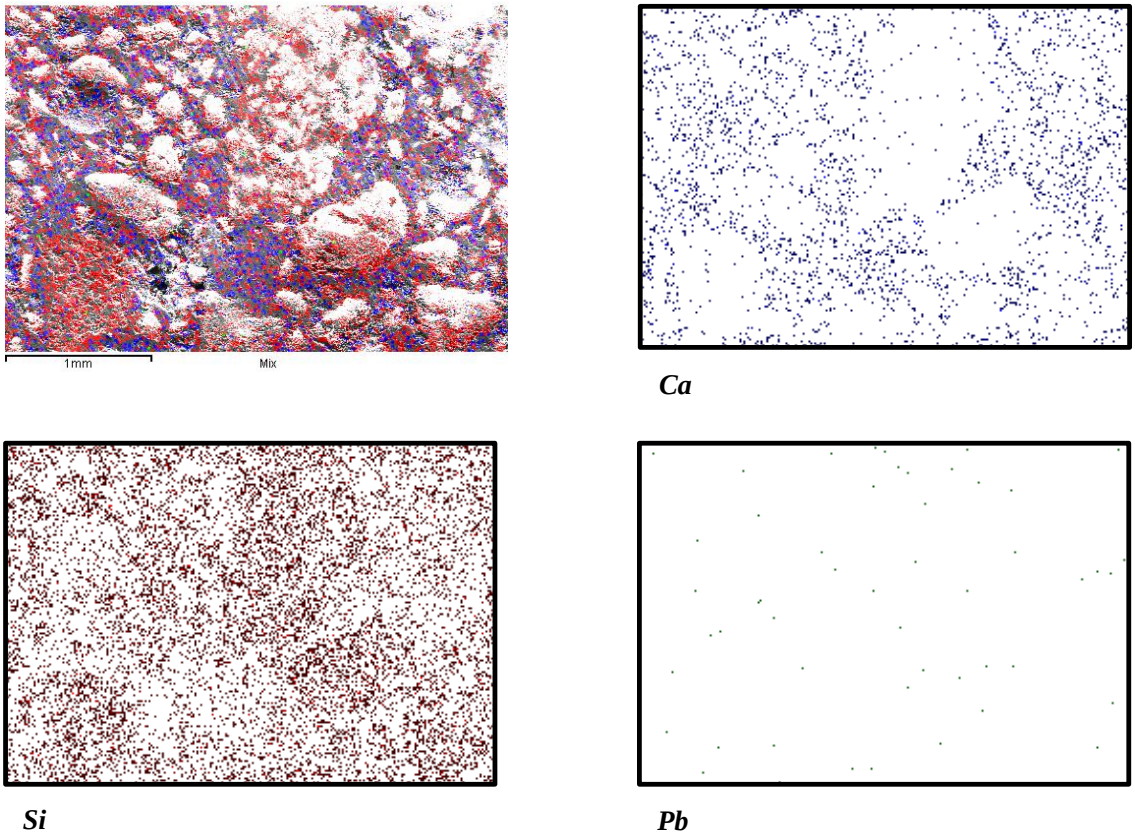

Figure 10. Pb-loaded cement mortar modified by LMWCH and X-ray mapping of Pb, Ca and Si. In the colored SEM image: brightest and red areas are Si-rich phases from the aggregate, embedded in the binding material, with blue points representing calcium. Distinct green points denote the presence of lead in the binding matrix.

Figure 11

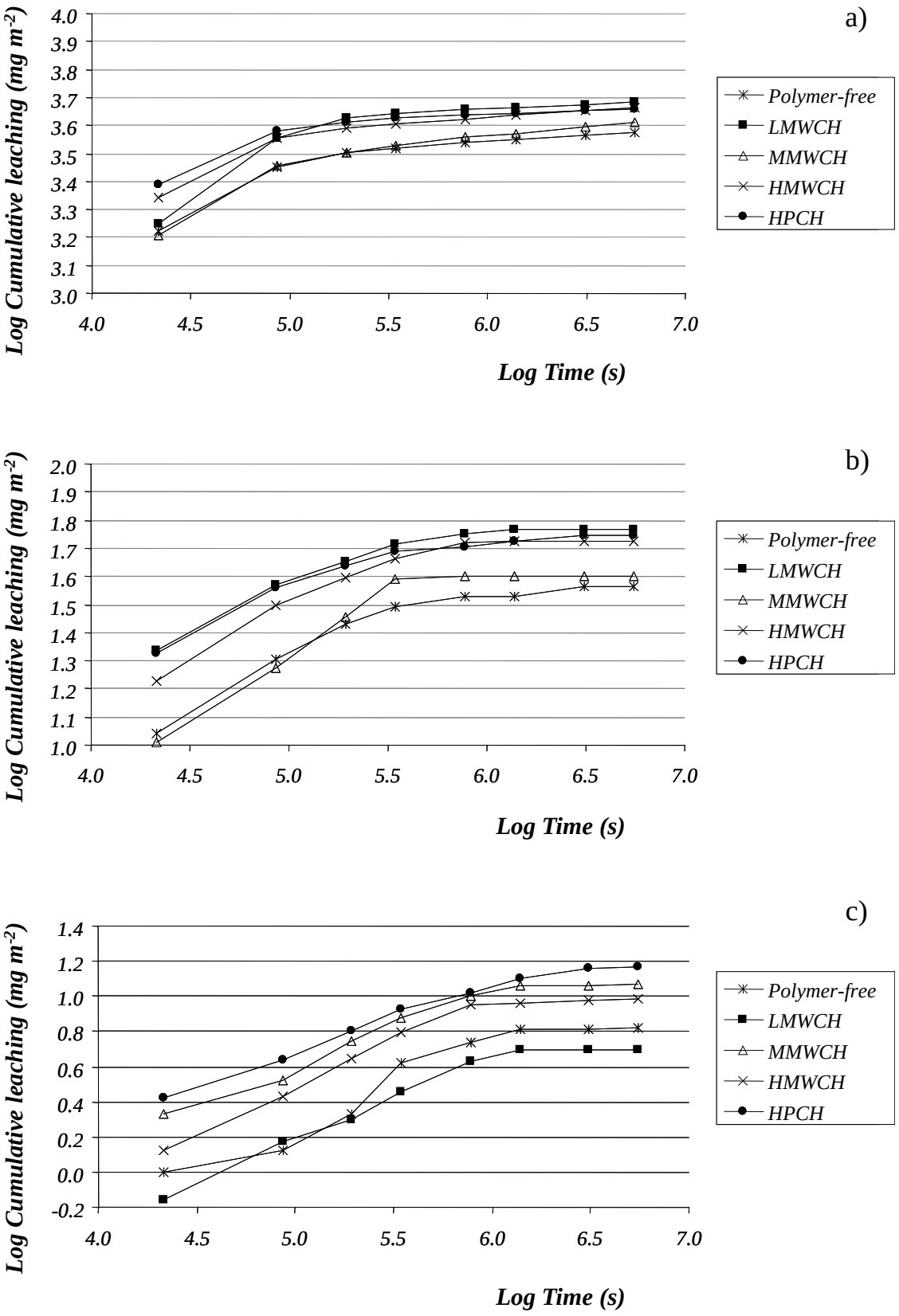

Figure 11. Log of cumulative leaching versus log of time for (a)Cr, (b) Pb and (c)Zn over 64 days.